UNIVERSITY OF TARTU

FACULTY OF SCIENCE AND TECHNOLOGY

INSTITUTE OF MOLECULAR AND CELL BIOLOGY

INSTITUTE OF BIOMEDICINE AND TRANSLATIONAL MEDICINE

DEPARTMENT OF PHARMACOLOGY

Kerli Tulva

Neuropathology and brain atrophy in Wolfram syndrome

Bachelor's Thesis

Gene Technology

12 EAP

Supervisor PhD Miriam Ann Hickey

Co-supervisor PhD Tambet Tõnissoo

TARTU 2017

ABSTRACT

Neuropathology and brain atrophy in Wolfram syndrome

Wolfram syndrome is a rare autosomal recessive disease. It is caused by mutations in the *WFS1* gene. The symptoms appear early in childhood including at first *diabetes mellitus* followed by optic nerve atrophy. Wolfram syndrome has currently no cure. Studies with patients have shown that most of atrophy occurs in the brain stem and cerebellum. Our work in the laboratory with the mouse model of WS has shown that the trigeminal nerve shows a critical role in disease progression. The aim of this work was to characterize very early changes in pathology in a mouse model of WS. In this thesis, I demonstrate how severely affected these mice are, by the time of initial brain changes detected using magnetic resonance imaging (MRI). The results showed that very young mice had a reduction in the cerebellar volume. The trigeminal tract size was also reduced. The used methods help to better understand early disease and to ultimately pinpoint earliest neurodegenerative changes for better management of these patients.

Keywords: Wolfram syndrome, *WFS1*, trigeminus, pons, cerebellum, histology

CERCS code: B640 Neurology, neuropsychology, neurophysiology

Wolframi sündroomi neuropatoloogia ja aju atroofia

Wolframi sündroom (WS) on haruldane autosomaalne retsessiivne haigus. See on põhjustatud mutatsioonidest *WFS1* geenis. Sümptomid avalduvad juba varajases lapseeas, mille esmaseks tunnuseks on suhkrutõbi. Sellele järgneb nägemisnärvi atroofia. Wolframi sündroomile tänaseni ravi puudub. Uuringutest patsientidega on leitud, et atroofia esineb kõige rohkem väikeajus ning ajutüves. Eelnevad katsed meie laboris WS hiiremudeliga on näidanud, et samuti kolmiknärvil on suur osa selle haiguse kulgemisel. Tuginedes varasematele andemetele WS kohta, püstitati antud bakalaureusetöö eesmärgiks välja uurida, kas WS põhjustab patoloogilisi muutusi *Wfs*$^{-/-}$ hiirte väikeajus, ajutüves ning kolmiknärvis juba enne, kui need muutused on magnetresonantstomograafia-ga (MRT) täheldatavad. Tulemustes selgus, et väga noortel hiirtel esineb väikeaju atroofia. Kahanenud oli ka kolmiknärvi trakt. Bakalaurusetöös saadud tulemused aitavad paremini mõista WS arengut ja seeläbi aidata patsiente, määrates täpselt kõige varajasemad neurodegeneratiivsed muudatused.

Märksõnad: Wolframi sündroom, *WFS1*, kolmiknärv, ajutüvi, väikeaju, histoloogia

CERCS kood: B640 Neuroloogia, neuropsühholoogia, neurofüsioloogia

CONTENTS

ABSTRACT 2

LIST OF ABBREVIATIONS 5

INTRODUCTION 6

1. LITERATURE REVIEW 8
   1.1 WOLFRAM SYNDROME 8
   1.2 GENETIC BACKGROUND OF WS 8
      1.2.1 *WFS1* AND *CSID2* 10
   1.3 SYMPTOMS AND DIAGNOSIS 10
   1.4 TREATMENT 12
   1.5 MOUSE MODEL OF WS 12
   1.6 BRAIN ABNORMALITIES IN WS 12
      1.6.1 BRAIN STEM AND CEREBELLUM IN WS PATIENTS 12
      1.6.2 BRAIN STEM AND CEREBELLUM IN WS MICE 14
      1.6.3 BRAIN STEM AND CEREBELLUM ANATOMY 14
      1.6.4 TRIGEMINAL SYSTEM IN WS PATIENTS 16
      1.6.5 TRIGEMINAL SYSTEM IN WS MICE 16
      1.6.6 TRIGEMINAL SYSTEM ANATOMY 17

2. EXPERIMENTAL 19
   2.1 THE AIM OF THE WORK 19
   2.2 MATERIALS AND METHODS 20
      2.2.1 ANIMALS 20
      2.2.2 BEHAVIOURAL ANALYSIS 20
      2.2.3 BRAIN STEM AND CEREBELLUM VOLUME ANALYSIS 21
      2.2.4 IMMUNOHISTOCHEMISTRY 22
      2.2.5 LUXOL FAST BLUE STAINING 22
      2.2.6 NEURONAL ANALYSIS OF THE TRIGEMINAL SYSTEM 23
      2.2.7 STATISTICS 24
   2.3 RESULTS AND DISCUSSION 24
      2.3.1 BEHAVIOURAL ANALYSIS 24
      2.3.2 BRAIN STEM AND CEREBELLUM ANALYSIS 25
      2.3.3 TRIGEMINAL TRACT ANALYSIS 28
      2.3.4 SOMA SIZE IN THE TRIGEMINAL MOTOR NUCLEUS 30
      2.3.5 DENSITY OF TRIGEMINAL MOTOR AND SENSORY NEURONS 30

CONCLUSION 32

KOKKUVÕTE 33
REFERENCES 35
ACKNOWLEDGMENTS 40
NON-EXCLUSIVE LICENCE 41

LIST OF ABBREVIATIONS

CSID2- Wolframin 2 gene
CSID2- Wolframin 2 protein
ER- endoplasmic reticulum
HET- heterozygous
KO- knock-out
moV- motor root of the trigeminal nerve
MBP- myelin basic protein
MRI- magnetic resonance imaging
P- pontine reticular nucleus
PBS- phosphate buffered saline
PFA- paraformaldehyde
P22- 22 day-old mice
sptV- spinal tract of the trigeminal nerve
TBS- tris-buffered saline
TMN- trigeminal motor neuron
TSN- trigeminal sensory neuron
V- trigeminal motor nucleus
VIIn- facial nerve
PSV- trigeminal sensory nucleus
Wfs1$^{-/-}$- knock-out mouse
Wfs1$^{+/-}$- heterozygous mouse
Wfs1$^{+/+}$- wild type mouse
WFS1- Wolframin gene (human)
Wfs1- Wolframin gene (mouse)
WFS1- Wolframin protein (human)
WFS1- Wolframin protein (mouse)
WS- Wolfram syndrome
WT- wild type

INTRODUCTION

Wolfram syndrome (WS) is a rare autosomal recessive disease. The *WFS1* gene resides in chromosome 4p16.1 and produces a protein called wolframin. The protein is best known to regulate calcium balance in the endoplasmic reticulum (ER). Defects in that gene cause WS as the ER becomes stressed leading to defects in mitochondrial dynamics (Cagalinec *et al*., 2016). It is known to damage in particular the beta-cells in the pancreas which have very high expression of wolframin protein (Urano, 2016). *Diabetes mellitus* is the first symptom of Wolfram syndrome, developing around the age of 5 in children (Chaussenot *et al*., 2011). Expression of this protein is also very high in some areas of the brain such as the brain stem and emerging human data shows very clear, very early loss in volume of pons in particular Hershey *et al*., 2012; Lugar *et al*., 2016).

Other abnormalities include optic nerve atrophy, deafness, renal tract abnormalities and *diabetes insipidus*. One of the most affected regions is the brain stem, and patients eventually develop dysphagia (difficulty in swallowing) and dyspnoea (difficulty in breathing) (Chaussenot *et al*., 2011). Patients often develop orofacial pain.

As there is no treatment for the disease and the best current method is a clinical monitoring and symptom relief for the patients, it is essential to develop new knowledge about the affected regions of the brain and carry out research to better understand how WS can be tackled. The disease being relatively rare, it is difficult to obtain sufficient patients. The Department of Physiology in the University of Tartu has developed a *Wfs1*$^{-/-}$ mouse model in order to further investigate the syndrome, and we are characterising its brain pathology in depth. Also, study of WS may shed light on other diseases caused by impaired mitochondrial dynamics.

Previous work in our laboratory has shown clear changes in brainstem and trigeminus in *Wfs1*$^{-/-}$ mice at late stages (1 year of age) and here I show that 8-month-old *Wfs1*$^{-/-}$ mice are already functionally impaired. Thus, I selected to study *Wfs1*$^{-/-}$ mice as early as possible to determine how soon disease-related neurodegenerative changes occurred. The experiments were done using neonatal mice. In order to understand the effect on brain stem, cerebellum and trigeminal nerve, histochemical, stereological and immunological methods were exploited. The total volume of the pons and cerebellum was measured and analysed. Furthermore, detailed characterisation of the trigeminus (myelin, neuronal density and tract size) was performed to understand the later changes that we have observed in these mice.

WS patients show significant atrophy in brain stem and cerebellum and often experience facial pain similar to trigeminal neuralgia. Recently, brain stem and trigeminal nerve atrophy was observed using MRI in older (8-month and 1 year old) *Wfs1*$^{-/-}$ mice in our laboratory. Therefore, the aim of this study was to detect the earliest brain pathology in neonatal *Wfs1*$^{-/-}$ mice based on previous information in WS patients and older *Wfs1*$^{-/-}$ mice.

1. LITERATURE REVIEW

1.1 WOLFRAM SYNDROME

Wolfram syndrome (WS) is also known as DIDMOAD and it was first described by Wolfram and Wagner in 1938 (Barrett and Bundey, 1997). WS is caused by mutations in the *WFS1* gene, which produces a protein called wolframin. It is membrane bound and resides in the ER (Takeda *et al*., 2001). It is an autosomal recessive disorder characterised by *diabetes mellitus* and *insipidus*, optic nerve atrophy and deafness. Only insulin-dependent *diabetes mellitus* and optic atrophy are necessary to diagnose the disease. In addition to these symptoms, patients develop neurological and psychiatric abnormalities (Barrett and Bundey, 1997). Wolframin protein deficiency induces ER stress which leads to inositol 1,4,5- triphosphate receptor dysfunction and disturbs calcium homeostasis, mitochondrial dynamics (mitophagy, fusion, fission and mitochondrial movements become dysfunctional) and causes delayed neuronal development *in vitro* (Cagalinec *et al*., 2016). Death normally occurs in the midlife due to respiratory failure as the brainstem shows extensive degeneration (Urano, 2016).

1.2 GENETIC BACKGROUND OF WS

WF is genetically inherited disease. It is heterogeneous and therefore can have multiple gene mutations which all cause the same phenotype. However, most mutations occur in the *WFS1* gene (Inoue *et al*., 1998). It is autosomal recessive which means it needs two mutated alleles for the disease to develop (see Fig. 1).

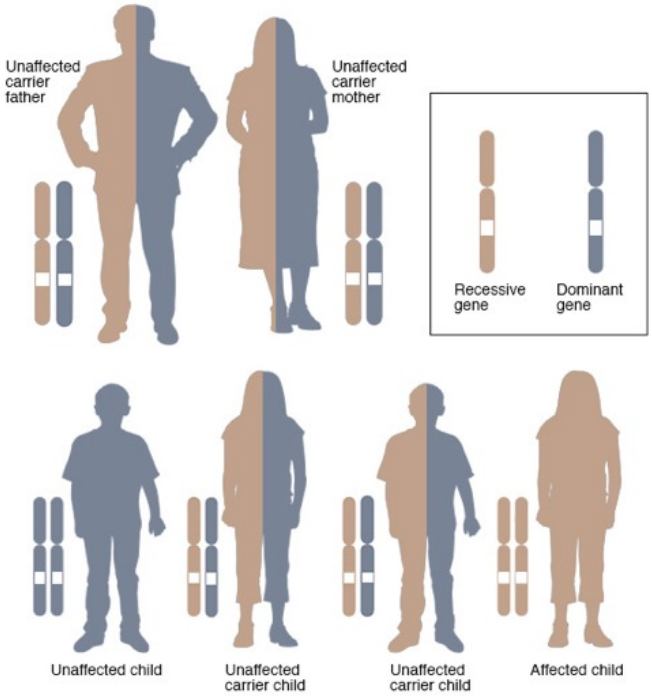

Figure 1. Autosomal recessive inheritance pattern. The mutated gene is inherited from both parents. There is 50% chance of being a carrier of the trait and 25% of having the disorder. If both dominant alleles are inherited (25%), the offspring will not pass the genes forward to the next generation (adapted from mayoclinic.org).

The *WFS1* gene is situated in chromosome 4 in p16 region in humans (see Fig. 2) and in chromosome 5 in qB3 in mice. The amino acid sequence identity in humans and mice is about 87% whereas the nucleotide sequence identity is about 83% (Strom *et al*., 1998).

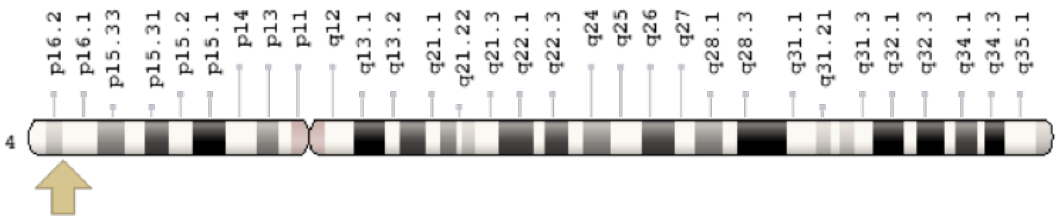

Figure 2. The location of the *WFS1* gene in humans. The *WFS1* gene is located in 4p16.1 position. (adapted from NCBI).

The WFS1 gene is 33.4 kb long (Inoue *et al*., 1998). It has eight exons (the coding regions of a gene) and most of the mutations causing WS occur in the 8th exon. This is also the largest exon and it contributes more than half of the protein-coding sequence (Cryns *et al*., 2003). The wolframin protein is 890 amino acids long (Hofmann *et al*., 2003). It is a 100kD, type II membrane protein which has nine helical transmembrane hydrophobic domains including N

and C hydrophilic parts (Strom *et al*., 1998). The protein is embedded in the ER and plays an important role in calcium homeostasis. Recently, we have shown that the loss of WFS1 protein in ER leads to the dysfunction of IP-3 calcium channel. This further causes ER stress and impaired mitochondrial dynamics (Cagalinec *et al*., 2016).

There are many different genetic mutations that can cause WS. The most common are 'loss of function' mutations, such as stop codons and frameshifts which constitute 40% of all cases. In addition, there are splice site and missense mutations which make up about 35% of the cases. The total number of mutations is approximately 200. However, there are no genotype-phenotype correlations and most of the patients are heterozygotes for their mutations (Rigoli *et al*., 2011).

The disease is very rare, having a prevalence only 1 in 770,000. However, the carrier frequency is estimated to be 1 in 3,542 meaning that there are many heterozygotes in the population carrying this mutation without themselves being affected (Boutzios *et al*., 2011).

1.2.1 *WFS1* AND *CSID2*

There are two types of Wolfram syndrome and both are autosomal recessive. The first type is caused by the mutations in *WFS1* gene as stated previously and the second one is caused by the mutations in *CSID2* gene. This encodes the CSID2 protein which resides in the outer membrane of ER but the precise function is unknown. Phenotypic differences are observed between these two types in which the latter one does not express the symptoms of *diabetes insipidus*. However, stomach ulcers and blood clotting difficulties are common (Mozzillo *et al*., 2014).

1.3 SYMPTOMS AND DIAGNOSIS

The clinical symptoms of WS patients include sensory-neural deafness, *diabetes insipidus*, *diabetes mellitus*, ataxia, psychiatric and neurological disorders, renal tract abnormalities and optic nerve dysfunction (Barrett and Bundey, 1997). *Diabetes mellitus* is the first characteristic which is observed at about 5 years of age. *Diabetes insipidus* appears later in the disorder at about 15 years of age. The median age for the start of neurological symptoms is at about 5 years (see Fig. 3) (Chaussenot *et al*., 2011). Investigation done by Pickett *et al*. identified significant gait impairments in very young WS patients including deficits in velocity and balance (Pickett *et al*., 2012). Patients with WS tend to have also sleep dysfunction as identified by Bischoff *et al*. but there is no evidence of cognitive impairment in WS (Bischoff *et al*., 2015).

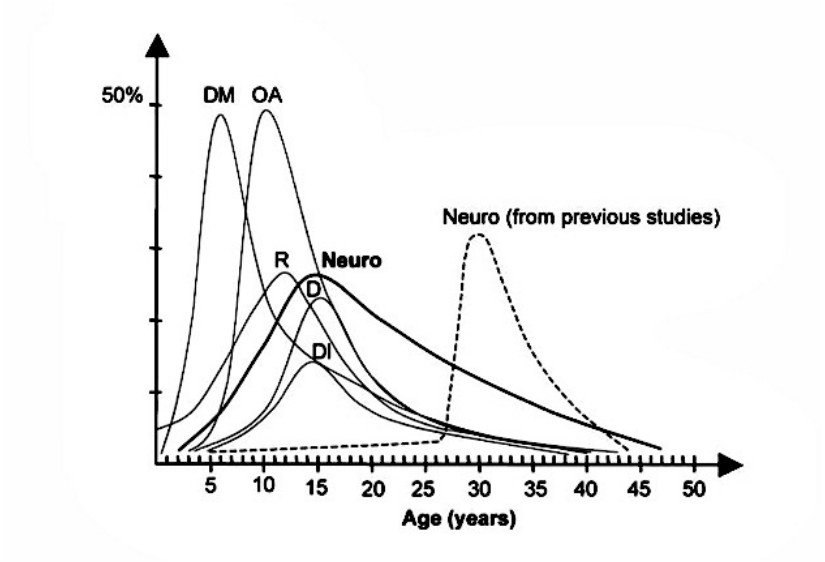

Figure 3. The median age (the peak) of each of the main characteristic symptoms of Wolfram syndrome. The dotted line represents the median age of neurologic complications in the Barrett's series. DM- *diabetes mellitus*; OA-optic atrophy; R- renal tract abnormalities; D- deafness; DI-*diabetes insipidus*; Neuro- neurologic complications (Barrett *et al* 1997; adapted from Chaussenot *et al*., 2011).

As mentioned earlier, the expression of wolframin is very high in pancreas. The absence of this protein leads to cell death in pancreatic beta-cells causing *diabetes mellitus* (Urano, 2016). *Diabetes insipidus* however, is caused by pituitary gland dysfunction (Rigoli *et al*., 2011).

The optic nerve atrophy is another diagnostic symptom of that syndrome which results in the loss of sight. Retinal nerve fiber layer (RNFL) thinning is often observed as an important marker (Hoekel *et al*., 2014). Children might also develop catharsis. Wolframin is expressed in retinal ganglion cells and photoreceptors which are essential for vision (Urano, 2016).

Deafness may be a symptom which starts in childhood and progresses over time. Karzon and Hullar conducted a research on hearing impairment in WFS patients and found that 55% of them had sensorineural hearing loss (Karzon and Hullar, 2013). About 62% of sufferers develop deafness (Hilson *et al*., 2009).

There are structural and functional renal tract abnormalities which may be partially caused by *diabetes mellitus* and *insipidus* as they affect the bladder dysfunction and upper urinary tract dilation. The bladder dysfunction is caused by the central and peripheral neurological dysfunction and further causes urinary tract infections in WS patients (Urano, 2016).

Central apnea and ataxia, both related to brain stem atrophy, are common neurological manifestations in WS patients. Autonomic and peripheral neuropathy are also commonly observed (Urano, 2016).

The minimal criteria for diagnosis are *diabetes mellitus* and optic atrophy, however genetic screening is necessary in order to confirm the phenotypical observations (Chaussenot *et al*., 2011). Neuroimaging is a good possibility to use in the future to detect altered brain stem and cerebellum abnormalities (Bischoff *et al*., 2015).

1.4 TREATMENT

Although the disease has no cure, the symptoms can be relieved. Diabetes, for example, can be relieved using contemporary treatment. However, the patients are known to only live until the age of 30-35 and death mainly occurs because of respiratory and swallowing problems due to brainstem failure (Hershey *et al*., 2012).

1.5 MOUSE MODEL OF WS

The *Wfs1*$^{-/-}$ mouse model used in the thesis was generated in the Department of Physiology, University of Tartu. They were generated by replacing the coding region of the *Wfs1* gene resulting in the deletion of 360-890 amino acids in the WFS1 protein (Luuk *et al*., 2009). Research done by Luuk *et al*. showed that homozygous *Wfs1*$^{-/-}$ mice have much lower body weight and higher blood glucose levels than WT mice. They also found that several measures of motor activities were diminished in *Wfs1*$^{-/-}$ mice and stressful environment conditions triggered anxiety-like behavior (Luuk *et al*., 2009).

In recent data, we revealed for the first time brain stem and optic atrophy in 1 year old *Wfs1*$^{-/-}$ mice (Cagalinec *et al*., 2016). Thus, these mice display several critical features of WS including the diagnostic features.

1.6 BRAIN ABNORMALITIES IN WS

1.6.1 BRAIN STEM AND CEREBELLUM IN WS PATIENTS

The current knowledge of the abnormalities in brains in WF patients come from clinical examination and *post mortem* case studies. Analyses done by Hershey *et al.* on brain stem volume of WS patients showed a significant decrease compared to healthy individuals.

Investigation of cerebellar grey and white matter showed a reduction. It was concluded from the results that a reduction in volume in brain stem and cerebellum is present from the earliest age yet analyzed (Hershey *et al*., 2012).

Those experiments were carried out on patients with Wolfram syndrome, healthy patients and patients with type 1 diabetes. The type 1 diabetes group was important to investigate the changes in brain volume caused by diabetic abnormalities only. Further investigation was done into the volume change in the three parts of brain stem. These data revealed that with the brain stem, pons was most affected (see Fig. 4) (Hershey *et al*., 2012).

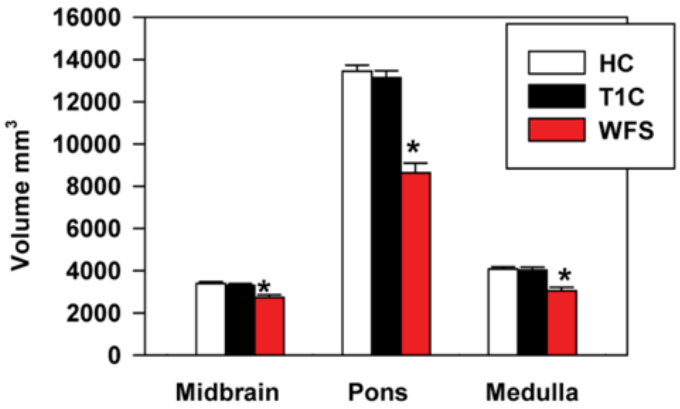

Figure 4. Volume of the three segments of the brain stem. The figure shows the results of Hershey *et al.* experiment with three groups of patients. HC stands for healthy person, T1C stands for type 1 diabetes and WFS stands for Wolfram syndrome patients. The reduction in pons volume is significant compared to the healthy and type 1 diabetes group. There is also slight volume reduction in medulla and midbrain (adapted from Hershey *et al*., 2012).

We can therefore conclude that the volume reduction of these parts of the brain occur quite early in childhood in humans. However, it remains unclear whether these changes occur from conception or develop over time.

The decrease in volume of the pons in particular has been suggested as a degenerative process by Lugar *et al.* as the abnormality increases with age. It was found that the ventral pons is more affected than the dorsal pons but both regions have a decrease in volume compared to the control groups. Ventral pons contains lots of white matter fibers and it is possible that the active demyelination of them is the cause of the decreased volume and the advancing abnormalities with age (Lugar *et al.,* 2016).

In the research conducted by Lugar *et al.* it was suggested that the degradation of myelin is the primary neuropathological symptom of Wolfram syndrome. Myelin surrounds the axons of the nerve cells and helps to speed up the electric signals from one neuron to another (Kiernan, 2007). The *WFS1* gene mutation induces endoplasmic reticulum mediated stress by interfering with the calcium homeostasis (Cagalinec *et al*., 2016). The myelinating cells are extremely sensitive to ER mediated stress as there is need to synthesize a large quantity of myelin proteins (Lin and Popko, 2009). The myelinating cell apoptosis might occur both in adulthood and in early development stages. Examinations of WS patients have found decreased myelin in the white matter in cerebellum and in ventral pons (Lugar *et al*., 2016).

Lugar *et al*. also analyzed brain stem fractional anisotropy (FA) (overall direction of water movement) and radial diffusivity (RD) (diffusion of water parallel to white matter fibers). The parameters showed a significant decrease in FA and increase in RD in most principal white matter tracts suggesting demyelination or lack of myelin around axons. The amount of myelin basic protein was also measured in the serum and an increased level was found in correlation of the progression of the disease, indicating an axonal damage (Lugar *et al*., 2016).

1.6.2 BRAIN STEM AND CEREBELLUM IN WS MICE

Recent work done by other personnel in our group (Cagalinec *et al*., 2016; Vdovenkova, Thesis, 2016) using MRI showed that *Wfs1*$^{-/-}$ mice at the age of 8 months and 1 year have reduced volume of the brain stem and trigeminus. Neonate mice showed no changes. However, the resolution of the images at this young age precludes detailed analysis.

The volume of the cerebellum was measured only in P22 mice with MRI and no significant decrease was detected. However, as we know the patients have shown a decrease in cerebellar volume and it is therefore necessary to investigate it more in depth with histology in the mouse model.

1.6.3 BRAIN STEM AND CEREBELLUM ANATOMY

The brain stem is located in caudal brain and is attached to the spinal cord and cerebellum (Fernandes-Gil *et al*., 2010). It consists of three main parts: midbrain, pons and medulla which carry the descending and ascending pathways for the cranial nerve nuclei (see Fig. 5). It controls the muscles of the head and regulates the perception of pain, movement, arousal, autonomic reflexes and consciousness (Hurley *et al*., 2010). The cranial nerves, reticular formation and

pontine nuclei form the grey matter and the white matter is made of nerve fibers. The internal part of the brainstem has also three divisions which are named tectum, tegmentum and basis. The tectum carries no cranial nuclei, tracts nor reticular formation whereas the tegmentum contains all the cranial nuclei. The basis has the motor pathways and also contains a lot of pontine nuclei at the level of the pons which has fibers projecting to the cerebellum (Fernandes-Gil *et al*., 2010).

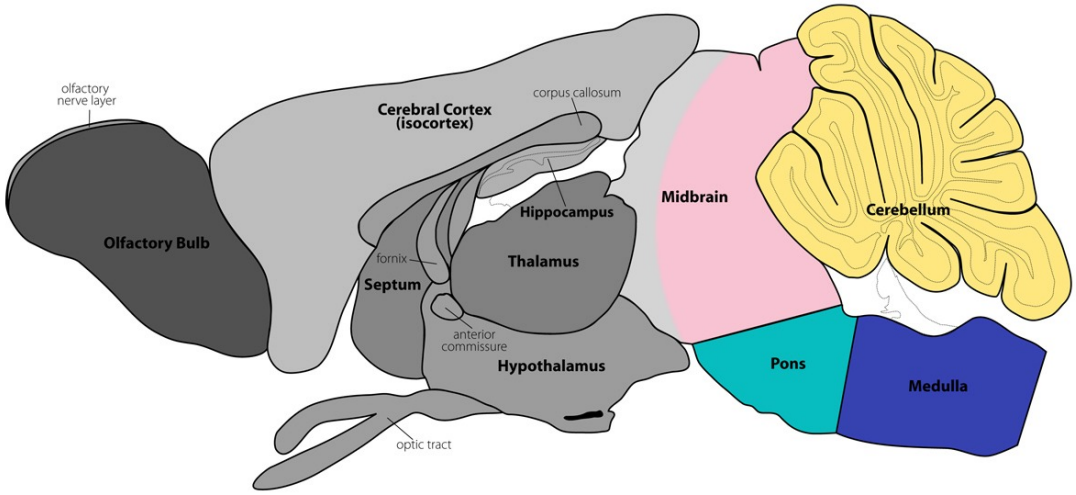

Figure 5. Three parts of the brainstem: midbrain, pons and medulla. A representation of a mouse brain. The midbrain is attached to the cerebellum (adapted from gensat.org).

The cerebellum coordinates muscle contraction and relaxation including muscle tone. The work of the cerebellum remains mainly under unconscious awareness (Kiernan and Rajakumar, 2014), for example swallowing and breathing are also controlled by it. Patients with Wolfram syndrome exhibit symptoms in the late stage related to the failure of the muscles in trachea and esophagus. They develop apnea (difficulty breathing) and ataxia (coordination and equilibrium problems) (Urano, 2016).

The cerebellum comprises the molecular and granular layer (grey matter) together with axons of passage in the white matter folium (see Fig. 6).

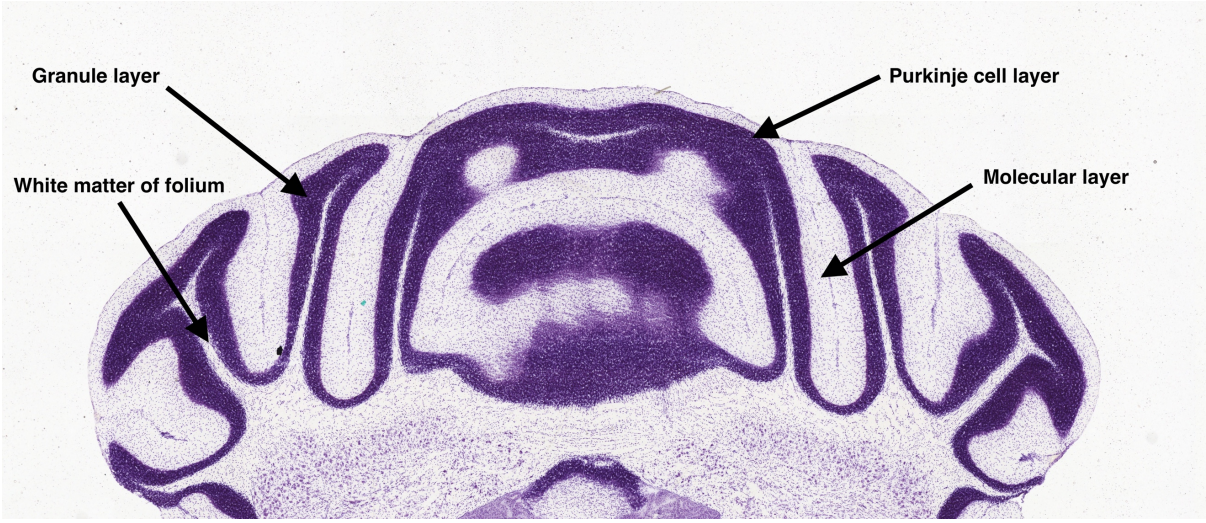

Figure 6. A cerebellum of a 56-day old mouse stained with Nissl. The somas of the Purkinje cells are found in the outer edge of the granular layer (adapted from Allen Brain Atlas).

1.6.4 TRIGEMINAL SYSTEM IN WS PATIENTS

It is known that some patients with Wolfram syndrome have facial pain, similar to trigeminal neuralgia. Trigeminal neuralgia is characterized by shock-like pain attacks and is caused by atrophy of the trigeminus e.g. loss of myelin (Montano *et al*., 2015). It is unclear what may cause the pain in WS. Some patients have difficulty swallowing and speech. These functions are controlled by cranial nerves (Urano, 2016). Swallowing in particular is controlled by the trigeminal system.

1.6.5 TRIGEMINAL SYSTEM IN WS MICE

Dr M. Hickey has demonstrated in previous experiments with 1 year old *Wfs1*$^{-/-}$ mice a reduction of trigeminal nerve volume using MRI. In further work Vdovenkova showed that this deficit was present in 8-month-old *Wfs1*$^{-/-}$ mice (see Fig. 7) (Vdovenkova, Thesis, 2016). MRI of neonate mice showed no atrophy. However, a major problem of MRI analysis of neonatal mice is the lack of white matter to enable good segmentation of different brain regions. Therefore here, I have used histological methods to examine these regions in detail.

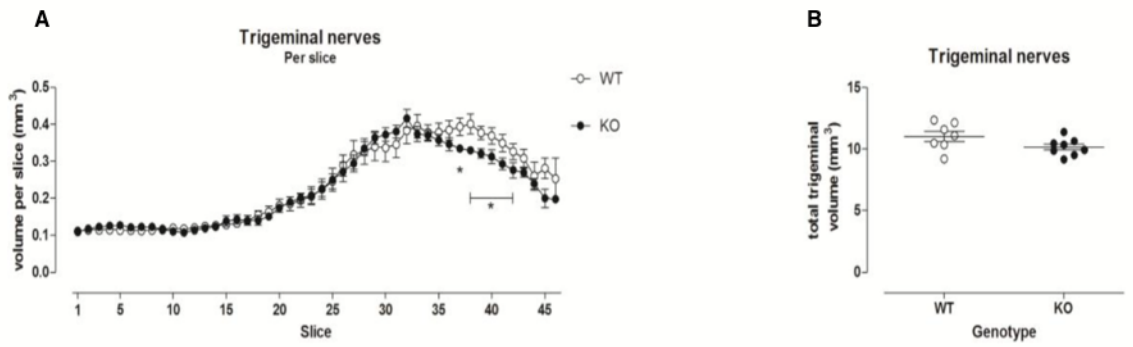

Figure 7. Trigeminal nerve volume from 8-month-old mice. Data was obtained by Vdovenkova using MRI. There is a reduction in volume seen in the motor and sensory parts of the trigeminal nerve (A; caudal (slices 36-42) areas show reduced volume per slice). However, total volume was not changed (B) (adapted from Vdovenkova, Thesis, 2016).

1.6.6 TRIGEMINAL SYSTEM ANATOMY

The trigeminal nerve is also known as the fifth cranial nerve, the largest of the cranial nerves. The trigeminal neurons are pseudounipolar; their axons receive sensory input from all aspects of the face, conjunctiva and cornea of the eye, nasal cavities, palate, temporomandibular joint, lower jaw, oral cavity and teeth. This information is sent, via the spinal trigeminal tracts, into the brain stem to 2nd-order neurons of the trigeminal sensory nucleus. From there, information is sent to the ventral posterior medial nucleus of the thalamus and then onto the somatosensory cortex. Functionally, the trigeminal nerve has three divisions: ophthalmic (V1), maxillary (V2) and mandibular (V3) (see Fig. 8). The first two have only a sensory component. The mixed mandibular branch (V3) is both sensory and motor, with trigeminal motoneuron axons exiting the pons via the spinal trigeminal tracts to innervate the muscles of mastication and swallowing (Bathla *et al.*, 2012; Patestas and Gartner, 2016).

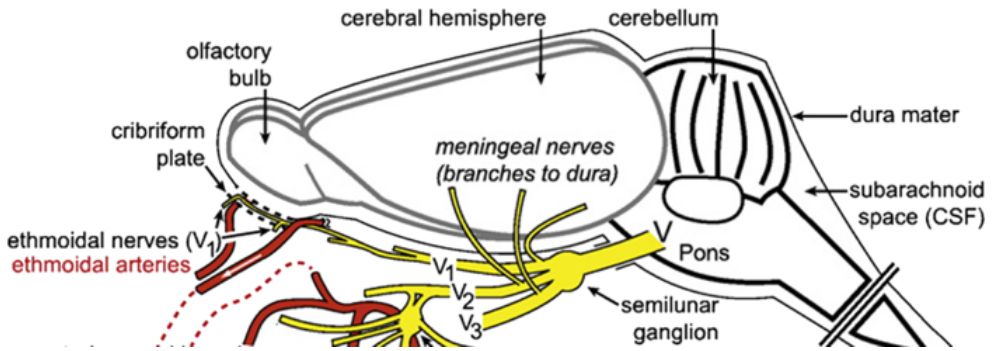

Figure 8. The three branches of the trigeminal nerve in a mouse. Shown in yellow there are three major sensory branches of trigeminal nerve: ophthalmic (V1), maxillary (V2) and mandibular (V3) system. The trigeminal tract enters the pons (adapted from Lochhead *et al*., 2012).

The mapping of the mouse trigeminal nerve study conducted by Erzurmulu *et al*. showed how the somatosensory circuits of the rodent face is organized. Facial somatosensory information goes to the brain through trigeminal circuit (see Fig. 9) (Bechara *et al*., 2015). Humans and mice have a very similar organization of trigeminal nerve except the fact that mice rely on whiskers for sensory input. The whiskers are innervated by the maxillary nerve on the upper jaw (Erzurmulu *et al*., 2010).

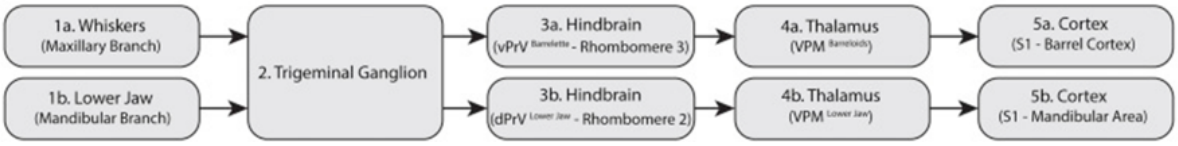

Figure 9. A representation of the mouse trigeminal circuit. Sensory signals received by the whiskers on the upper jaw (maxillary branch) and by the lower jaw (mandibular branch) are processed in trigeminal ganglion. From there they pass through the hindbrain and thalamus to the cortex (adapted from Bechara *et al*., 2015).

The trigeminal motor and sensory nuclei reside in lateral pons. The sensory nucleus (also called the principal sensory nucleus) resides laterally to the motor nucleus. They are separated by the motor root of the trigeminal nerve (see Fig 10). The somas of the motor neurons are much larger than the sensory neurons of the sensory nucleus.

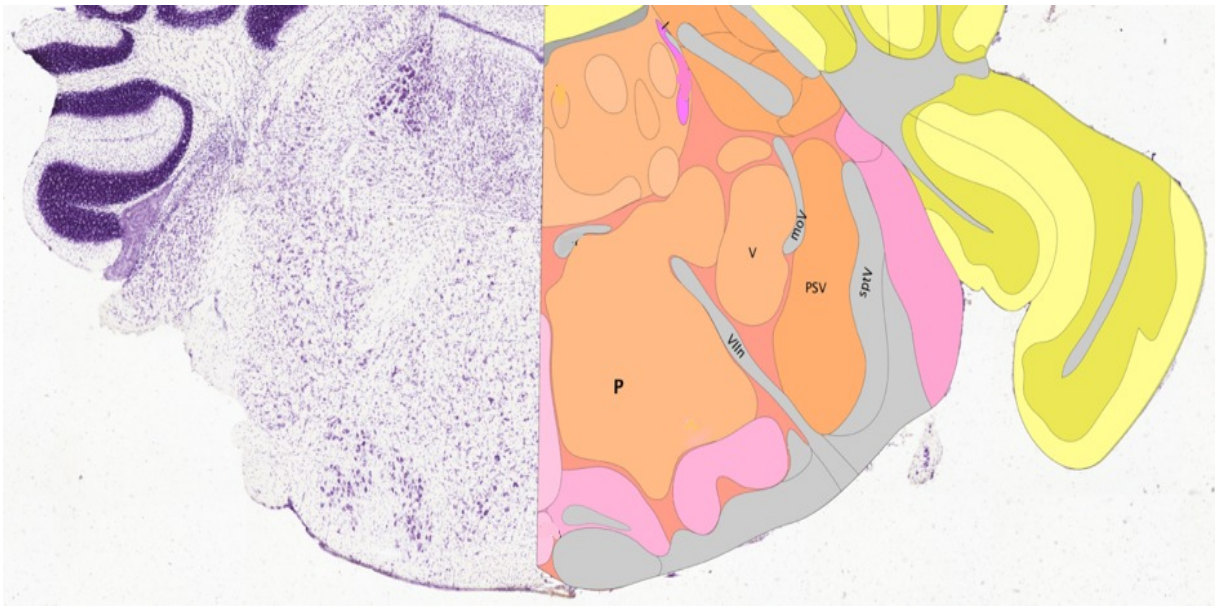

Figure 10. A coronal section of brainstem from a 56-day-old mouse. The motor nucleus (V) resides in lateral pons. It is easily identified in coronal and sagittal planes when stained with Nissl as the neurons in this nucleus have very large cell bodies. The motor nucleus is separated from the principal sensory nucleus by the motor root of the trigeminal nerve (moV). The nucleus is also surrounded by pontine reticular nucleus (P) and facial nerve (VIIn) (Kostakis *et al*., 2008). The PSV resides laterally to the V and is much larger. It is surrounded by the spinal tract of the trigeminal nerve (sptV), moV and the VIIn. The neural cell bodies are much smaller compared to the V (adapted from Allen Brain Atlas).

2. EXPERIMENTAL

2.1 THE AIM OF THE WORK

Our research group is investigating the mouse model of Wolfram syndrome. Previously it has been shown in our lab using MRI that there is progressive atrophy in specific parts of the brain and nerve tracts. The aim of this study was to investigate very early brain pathology of P22 *Wfs1*$^{-/-}$ mice and compare them to their WT littermates by using histological and microscopic methods to understand changes in more detail.

The specific aims were:

1. To analyze the behavior and activity of 8-month-old *Wfs1*$^{-/-}$ and WT mice to determine how severe their disease progression was at that age.
2. To measure the volume of the brainstem and cerebellum of P22 *Wfs1*$^{-/-}$ and WT mice to determine if changes in volume or white matter were present at that young age.
3. To investigate changes in the trigeminal tract in the brain stem of P22 *Wfs1*$^{-/-}$ and WT mice by examining myelin content in brain stem, neuronal morphology and trigeminal tract size.

2.2 MATERIALS AND METHODS

2.2.1 ANIMALS

For this work 8-month and 22-day-old (P22) male mice were used (as it takes longer to see symptoms in females). The 8-month-old mice were used as by that age, *Wfs1*$^{-/-}$ have shown a decrease in brain stem and trigeminal nerve volume using *ex vivo* MRI. The 22-day-old mice were used for histological analyses as this was the earliest possible age. Heterozygote (HET) *Wfs1*$^{+/-}$ mice were bred to obtain *Wfs1*$^{+/+}$ (WT), *Wfs1*$^{-/-}$ (KO) and *Wfs*$^{+/-}$ (HET) littermates from which WT and *Wfs1*$^{-/-}$ only were used for the analysis (F2 hybrids ([129S6/SvEvTac × C57BL/6] × [129S6/SvEvTac × C57BL/6])). The number of P22 mice were as follows: *Wfs1*$^{-/-}$ n=6 and WT n=4. The 8-month-old mice were as follows: *Wfs1*$^{-/-}$ n=10 and WT n=8.

Mice were housed under standard laboratory conditions on a 12- hour light and dark cycle with free access to food and water.

Brains were prepared from mice who were anesthetized and transcardially perfused with 0.1M phosphate-buffered saline (PBS) at 37°C, then fixed with 4% paraformaldehyde (PFA) solution at 4°C. The brains were dissected out, placed in 4% PFA overnight and then in 30% sucrose for cryoprotection. Brains were placed in Eppendorfs and then frozen in liquid nitrogen. Once frozen, they were stored at -80°C until processing.

Experiments were approved by the University of Tartu Ethics committee, Loomkaitseprojekti Loakomisjon (nr. 68), according to EU Directive 2010/ 63/ EU. The perfusions were performed by Dr. MA Hickey who is authorized to perform this work.

2.2.2 BEHAVIOURAL ANALYSIS

8-month-old mice were videotaped by MA Hickey, who is licenced to perform animal experiments. Video analysis was conducted by me in Biomedicum. Each mouse was analysed for 5 minutes and its behaviour noted. The criterion for rearing was 1 or 2 paws off the ground (not grooming). The criterion for climbing was four paws off the ground (see Fig. 11). Initial training runs were performed to ensure that I gained a minimum threshold of accuracy.

Figure 11. **Behavioural analysis in 8-month-old mice.** WT mice are shown. On the left, a climbing mouse (all four paws off the ground) is shown. On the right, a rearing mouse (two paws off the ground) is shown.

2.2.3 BRAIN STEM AND CEREBELLUM VOLUME ANALYSIS

Stereological methods were used to accurately estimate volume. The brains of the *Wfs1*$^{-/-}$ and WT mice were coronally-sectioned at 35 microns at the level of brain stem and cerebellum covering the entire object of interest. The sectioning was performed in SIME by Dr. MA Hickey. For histological analysis, starting from the most caudal section, every 7th section was picked until the entire object of interest was covered. The sections were washed in 0.01M phosphate-buffered saline (PBS) for 5 min, then 3x in 0.1M tris-buffered saline (TBS) 5 minutes per wash. They were mounted on glass microscope slides. The sections were stained with cresyl violet (Acros Organics). Standard cresyl violet staining protocol was used (Hickey *et al*., 2008). Briefly the sections were immersed in distilled water (dH_2O) for 3 min. They were then incubated in cresyl violet for 5 min. Then, they were washed briefly in dH2O and differentiated in 70% alcohol containing 1% glacial acetic acid, and further dehydrated in 96% ethanol. Sections were cleared in Histochoice (Sigma Aldrich), mounted in resin (DPX; Sigma Aldrich) and covered with coverslips (see Fig. 12).

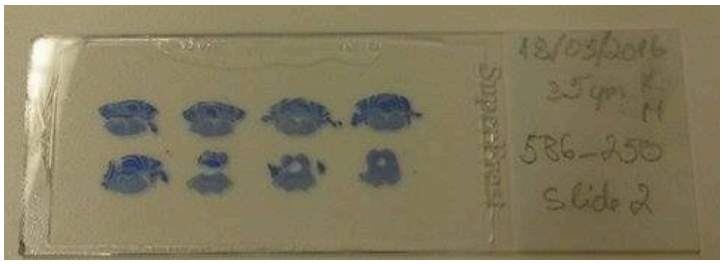

Figure 12. **Example of cross-sections of mouse brain stained with cresyl violet.** Due to the number of sections per mouse, 2 slides per mouse were used.

Stereo Investigator software (MBF Bioscience, Williston, VT, USA) was used to determine the volumes at 5x magnification. The area of brain stem and cerebellum in each section from every series was calculated by the software and volume obtained by multiplying by the factor 350 μm (7x35μm). All analysis was conducted by myself blinded to genotype.

2.2.4 IMMUNOHISTOCHEMISTRY

Two sections at approximately the same Bregma level (-6.255mm) containing cerebellum and brain stem were picked from each mouse. They were washed 3x in 0.01M PBS. Sections were blocked in 0.01M PBS, 1% BSA and 0.5% Triton-X. The sections were incubated while rocking at room temperature for 30 minutes. Sections were then incubated overnight at 4°C on a moving rack in primary antibody (1:50, rabbit anti-myelin basic protein, Sigma-Aldrich catalogue no. M3821) They were then washed 3x 5 minutes with 0.01M PBS containing 0.5% Triton-X. Sections were then exposed to secondary antibody (1:200, goat anti-rabbit IgG, ThermoFisher Scientific) for 2 h in the dark. Sections were then washed (3x 5min 0.01M PBS containing 0.5% Triton-X) and mounted on glass slides using Vectashield (Vector Laboratories), for analysis. Pictures were taken with Stereo Investigator software and optical density was measured using ImageJ. All pictures were taken at the same settings to ensure consistency. The control (with no primary antibody) showed no specific staining, hence it was not possible to take a picture at 20x magnification (too dark).

2.2.5 LUXOL FAST BLUE STAINING

Two sections from each mouse were chosen at the level of trapezoid body, trigeminal tract and facial nerve to get very similar location between the mice (-5.655mm from Bregma). They were washed in 0.01M PBS for 5 min and in 0.1M TBS 3x for 5 min. Sections were mounted on glass microscope slides and stained overnight with Luxol Fast Blue at 60°C. They were washed in 70% ethanol and then in distilled water. After that the sections were placed in lithium carbonate for 15 minutes and then rinsed quickly in 70% ethanol for 3x. Lastly, they were immersed quickly 2x in cresyl violet and then mounted using DPX (ThermoFisher).

Photomicrographs (brightfield) were taken for analysis (ZEN 2 Carl Zeiss Microscopy GmbH, 2011). The optical density and the size of trigeminus was measured by delineating the area of the trapezoid body (included as it was not possible to discriminate on LFB-stained sections) and trigeminal tract using ImageJ (W. Rasband, USA, version 1.8.0_66).

2.2.6 NEURONAL ANALYSIS OF THE TRIGEMINAL SYSTEM

The stereological series of cresyl violet stained sections was used for this work. All sections containing the trigeminal motor nucleus (TMN) and trigeminal sensory nucleus (TSN) were identified (see Fig. 13). These TMN and surrounding TSN were then analysed for 1) area (TMN, TSN), 2) neuronal soma size (TMN), 3) neuronal density (TMN, TSN).

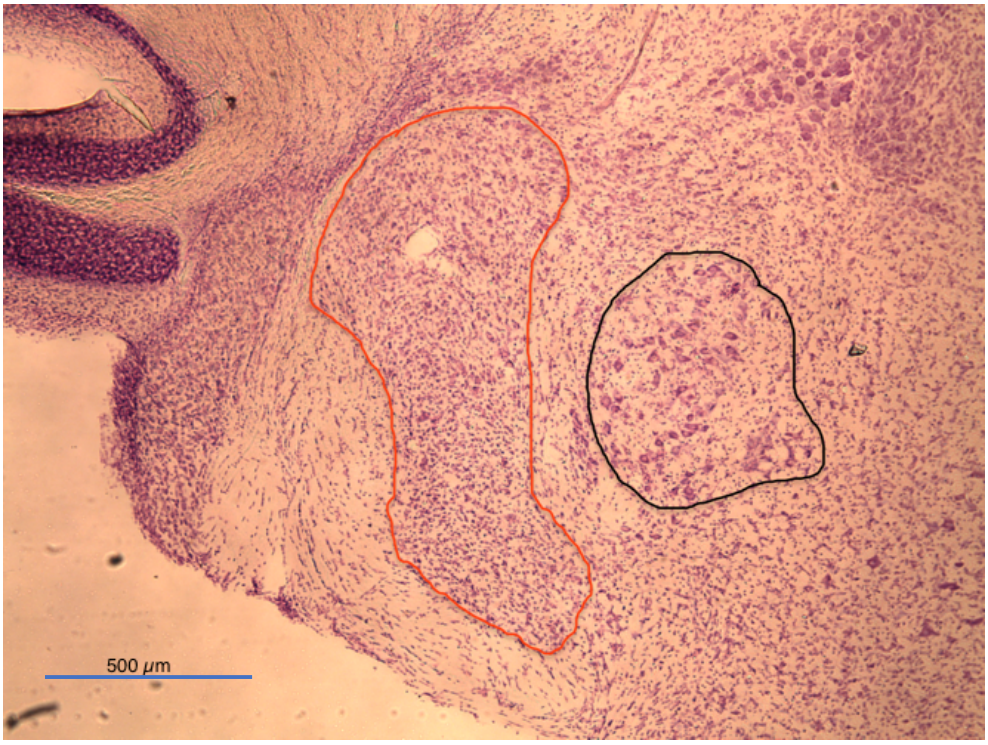

Figure 13. An 5x image from a P22 mouse brain stem stained with cresyl violet. The red contour represents the area of the trigeminal sensory nucleus and the black contour represents the trigeminal motor nucleus (note the much larger neurons in this nucleus).

The size of the neuronal soma (TMN) was measured by delineating the area of each cell body using ImageJ (W. Rasband, USA, version 1.8.0_66).

Estimates of trigeminal sensory neuronal number were obtained using non-biased methods with Stereo Investigator (MBF Bioscience, Williston, VT, USA version 11.02) at 63x magnification (counting frame size 30 microns, grid size 180 microns). Estimates were obtained for every nucleus. For the motor nucleus, all neurons within every nucleus was counted. The area of the sensory and motor nucleus was measured using Stereo Investigator at 5x magnification. Density of neurons, per mm^2, was then calculated per hemisphere, then per section, then per mouse in order to obtain group means (a minimum of 2 sections per mouse).

2.2.7 STATISTICS

Mean values +/- standard error of the mean (mean ±SEM) was used to present all of the data. The critical value was set to 0.05. Student t-tests were used for the data analysis. Mann-Whitney U-test was used for the behavior analysis. The program used was Prism (version 5).

2.3 RESULTS AND DISCUSSION

I first examined the extent of disease progression in older *Wfs1*$^{-/-}$ mice. Having established the severity of disease in these older mice, I then examined very early brain abnormalities in P22 *Wfs1*$^{-/-}$ mice.

8-month-old and 22-day-old mice (P22) were analyzed. 8-month-old mice were used for behavioral analysis because by that age mice have shown significant changes in brain stem and trigeminal volume, in *ex vivo* MRI studies. P22 mice were used for all of the histology experiments as this was the earliest possible age for analysis.

2.3.1 BEHAVIOURAL ANALYSIS

In 8-month-old *Wfs1*$^{-/-}$ mice, body weight (g) showed a vast reduction compared to WT littermates (almost 50%). However, there was no difference in body weight of P22 mice (Student's t-test, $p>0.05$). The 8-month-old mice showed significant brain stem atrophy and trigeminal atrophy, previously observed with MRI (Vdovenkova, Thesis, 2016), so it was necessary to observe the extent of disease in mice of this age.

There was a very significant reduction in rearing and climbing in *Wfs1*$^{-/-}$ mice (see Fig. 14). Previous research done by Luuk *et al*. showed a decrease in body weight, anxiety-like behaviour in stressful environments and a reduction in rearing in 2-4 months old mice. It was suggested that WFS1 protein plays a major role in behavioural adaption (Luuk *et al*., 2009). The reduction in climbing here may be due to a lack of motivation to explore. Dopamine is an important neurotransmitter which plays a role in reward-motivated behaviour. Lack of dopamine leads to more anxiety-like behaviour and a decrease in motivation. It was suggested by Visnapuu *et al*. that WFS1 affects the release of dopamine (Visnapuu *et al*., 2013). It is also possible that reduced motor coordination plays a role, as mouse models of Huntington's disease show severe deficits in climbing from a young age (Hickey *et al*., 2005, 2008). Thus, at the age where we

therefore have observed trigeminal and brain stem atrophy, mice are severely impaired, warranting analysis of younger mice.

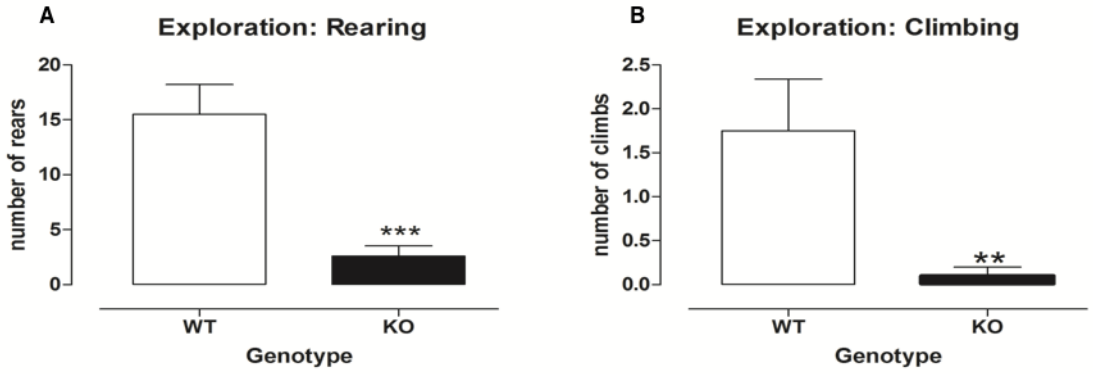

Figure 14. Rearing and climbing analysis. *Wfs1*$^{-/-}$ mice show a significant reduction in rearing (A) and climbing (B). WT vs *Wfs1*$^{-/-}$, *** p<0.01, Mann-Whitney U test, **p<0.01, Mann-Whitney U test. WT n=8, *Wfs1*$^{-/-}$ (KO) n=10.

2.3.2 BRAIN STEM AND CEREBELLUM ANALYSIS

Human data has shown that brain stem (especially pons) is affected by WS and the volume significantly reduced in young children (Hershey *et al*., 2012; Lugar *et al*., 2016). Brain stem dysfunction leads to respiratory failure or dysphagia which is the main cause of early death in WS (Chaussenot *et al*., 2011). It is therefore important to use mouse model of WS to investigate brain volume abnormalities and detect the earliest possible changes.

The volume of the brain stem was not significantly reduced in P22 *Wfs1*$^{-/-}$ mice when examined with MRI (Vdovenkova, Thesis, 2016). Similarly, no loss in total brain stem volume was observed in P22 *Wfs1*$^{-/-}$ mice using stereological analysis (see Fig. 15). These data confirm that brain stem degenerates as the mice age, but develops normally. This also confirms the data from Lugar *et al*. showing that the pons volume of WS patients decreases as they age (Lugar *et al*., 2016).

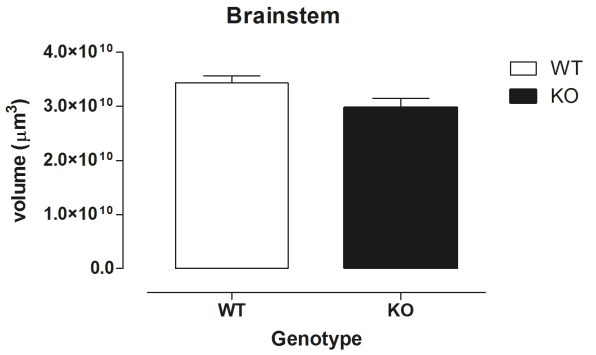

Figure 15. Total brain stem volume. The total volume of the brain stem is not significantly reduced in *Wfs1*$^{-/-}$ mice compared to their WT littermates therefore suggesting a degenerative process as the mice age (Student's t-test, p>0.05). WT n=4, *Wfs1*$^{-/-}$ (KO) n=6.

MRI analysis of cerebellar volume in P22 *Wfs1*$^{-/-}$ mice showed no reduction (Vdovenkova, Thesis, 2016). However, cerebellar volume is reduced in WS patients at an early age (Hershey *et al*., 2012; Pickett *et al*., 2012). Cerebellum is important in controlling gait and it is known from previous research that WS patients exhibit gait impairment (Pickett *et al*., 2012). Using histology, I found that there is quite a significant reduction in total cerebellar volume of P22 *Wfs1*$^{-/-}$ mice (see Fig. 16, *p<0.03). This can be either due to loss in axons (white matter; myelin reduction, axon degeneration) or grey matter (cell body reduction, e.g., Purkinje cells or granule cells). At this early age, it suggests that the reduction in cerebellar volume might be a developmental process.

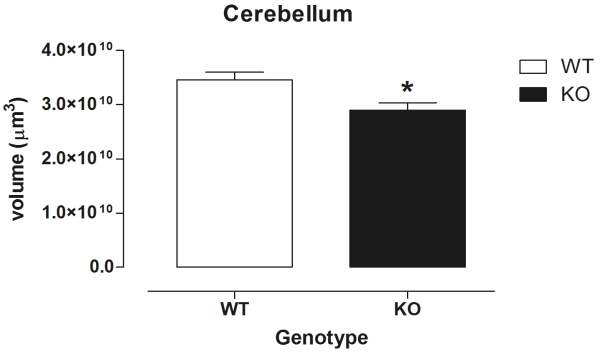

Figure 16. Total cerebellar volume. There was a statistically significant reduction in total cerebellar volume in P22 *Wfs1*$^{-/-}$ mice compared to their WT littermates (*p<0.03, Student's t-test). WT n=4, *Wfs1*$^{-/-}$ (KO) n=6.

To understand the reduction in total cerebellar volume in more detail, we next examined myelin basic protein (MBP) expression in cerebellar folia. It is known from previous research in patients (Lugar *et al*., 2016) and in another mouse model of WS (Lu *et al*., 2014) that there is

an increase in the myelin basic protein in the serum (patients) and in the brain lysate (in mice), suggesting axonal damage. Fluorescence optical density from sections labelled with anti-MBP was measured and a significant reduction was noted in *Wfs1*$^{-/-}$ mice compared to WT littermates (see Fig. 17; 18). Therefore, myelin reduction is likely contributed to the loss in total cerebellar volume. This suggests that myelin is degenerated in the cerebellar white matter and confirms the findings of Lugar *et al*. (2016). Our data suggests that the myelin is degenerating already at a very early age in cerebellum.

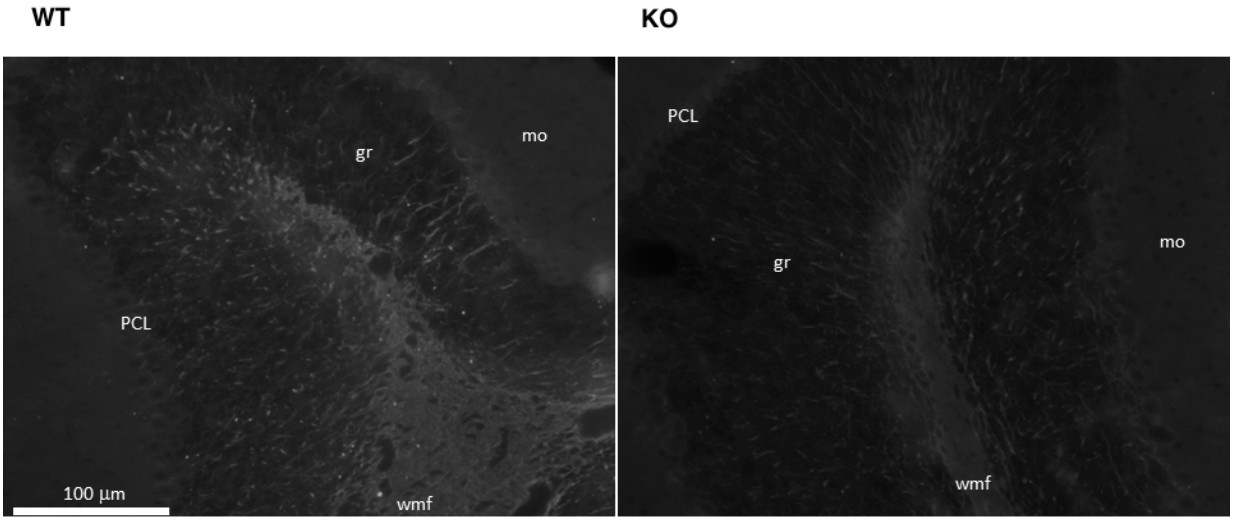

Figure 17. Cerebellar cryosections stained for myelin basic protein. PCL- Purkinje cell layer, gr- granular layer, mo- molecular layer, wmf- white matter of folium.

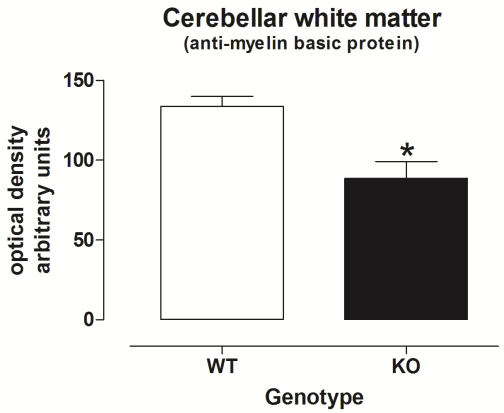

Figure 18. Myelin basic protein expression in cerebellar white matter. Myelin basic protein expression in cerebellar white matter (folium), detected using fluorescence immunocytochemistry, was significantly reduced in *Wfs1*$^{-/-}$ mice ($P<0.02$, Student's t-test). WT n=4, *Wfs1*$^{-/-}$(KO) n=6.

In future, it will be necessary to investigate axons and cell bodies in the cerebellum in more detail. For example, Purkinje cells, in the outermost layer of the molecular layer of the cerebellum show a high expression of wolframin (Luuk *et al*., 2008).

2.3.3 TRIGEMINAL TRACT ANALYSIS

Given the changes in trigeminal nerve (the trigeminus, cranial nerve V) observed in older mice (8-month and 1 year old), it was very important to conduct more detailed research using histological techniques of the spinal trigeminal tract, where the axons of passage of the trigeminal neurons enter the pons and axons of the trigeminal motor neurons exit the pons. The trigeminal tract comprises the axons of the trigeminal neurons which receive sensory information from the three divisions from the face. Those axons synapse with the trigeminal sensory neurons of the trigeminal sensory nucleus in the pons. The trigeminal motor neurons of the trigeminal motor nucleus send their axons via the trigeminal tract to the trigeminus and ultimately to innervate the jaw and enable mastication. WS patients show deficits in swallowing and speech and headaches and trigeminal neuralgia-like pain is also common (Urano, 2016).

I found a reduction in the area of the trigeminal tract in P22 *Wfs1*$^{-/-}$ mice compared to WT littermates (see Fig. 19). This suggests that there might be a reduction in trigeminal nerve axons (including myelin). However, it may also be due to a reduction in axons exiting the trigeminal motor nucleus. Thus, I went on to examine these important nuclei in more detail, as they are known to express WFS1 (Luuk *et al*., 2008).

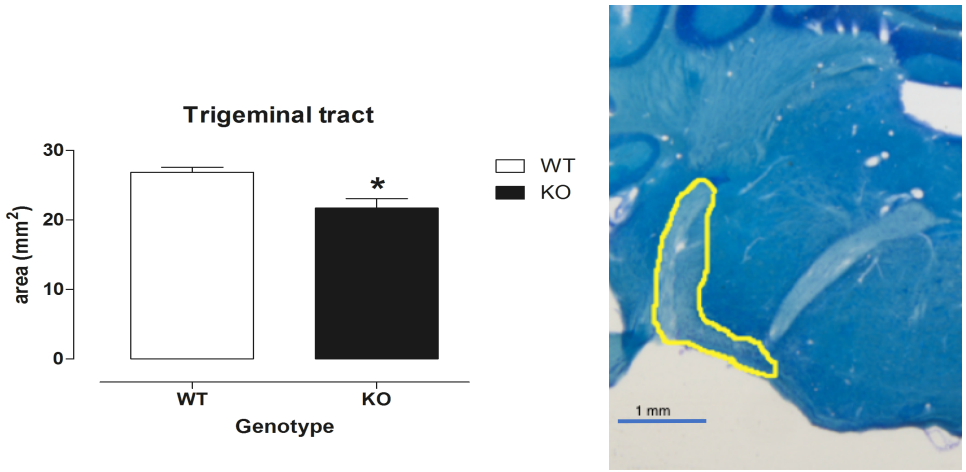

Figure 19. Spinal trigeminal tract area. A reduction in the spinal trigeminal tract area (trapezoid body also included) was observed in P22 *Wfs1*$^{-/-}$ mice (Student's t-test, *p<0.05). WT n=4, *Wfs1*$^{-/-}$ (KO) n=5. On the right, a section from a P22 mouse stained with Luxol Fast Blue. The trigeminal tract is delineated in yellow for area and optical density analysis. The facial nerve is seen medial from the tract and was used as a landmark to obtain sections at the same Bregma level (-5.655mm).

Optical density measurements of Luxol Fast Blue of the trigeminal tract was measured to investigate myelin content. No difference was detected between *Wfs1*$^{-/-}$ and WT mice (see Fig. 21, A). Since immunohistochemical staining for MBP is a more sensitive measure of myelin (Vincze *et al*., 2008), the optical density of fluorescently labelled anti-MBP were also quantified, in more caudal sections (see Fig. 20). Optical density confirmed no significant reduction in myelin basic protein in the tract (see Fig. 21, B).

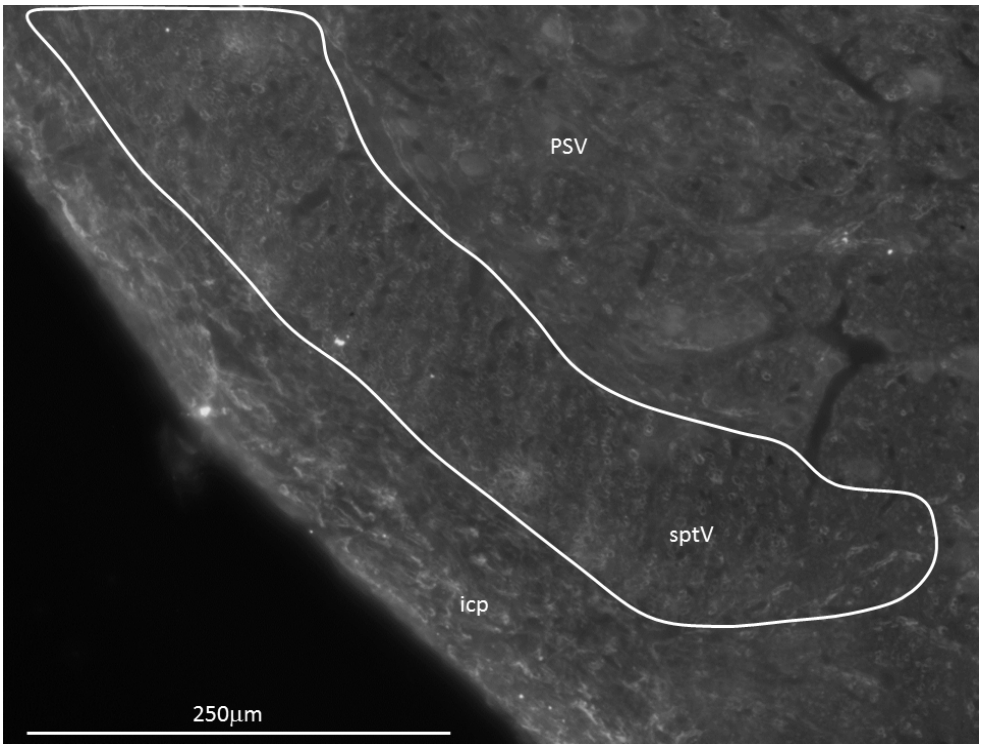

Figure 20. Spinal trigeminal tract stained immunohistochemically for myelin basic protein. PSV- principal sensory nucleus, sptV- spinal trigeminal tract, icp- inferior cerebellar peduncle.

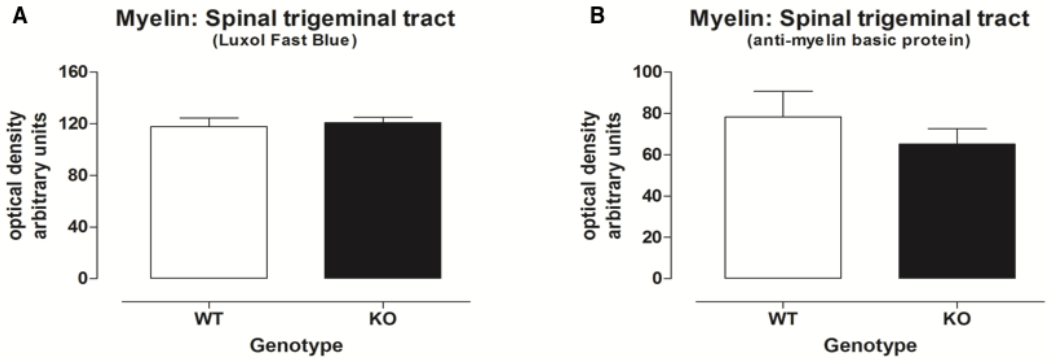

Figure 21. Myelin content in spinal trigeminal tract stained with Luxol Fast Blue (A) and stained with anti-MBP (B). Myelin content in P22 *Wfs1*$^{-/-}$ mice showed no reduction compared to WT littermates. For the Luxol Fast Blue: WT n=4, *Wfs1*$^{-/-}$ (KO) n=5. For the myelin basic protein: WT n=4, *Wfs1*$^{-/-}$(KO) n=6.

2.3.4 SOMA SIZE IN THE TRIGEMINAL MOTOR NUCLEUS

Given the involvement of TMN axons in the spinal trigeminal tract, and their high-intensity expression of WFS1, I also investigated cell body (soma) size of the trigeminal motor nucleus. A frequency distribution of soma size was conducted (see Fig. 22, A) Most of the cells were 0.004-0.006 mm^2 and no significant difference was observed between *Wfs1*$^{-/-}$ and WT mice, although a trend towards smaller cells was noted in *Wfs1*$^{-/-}$ mice.

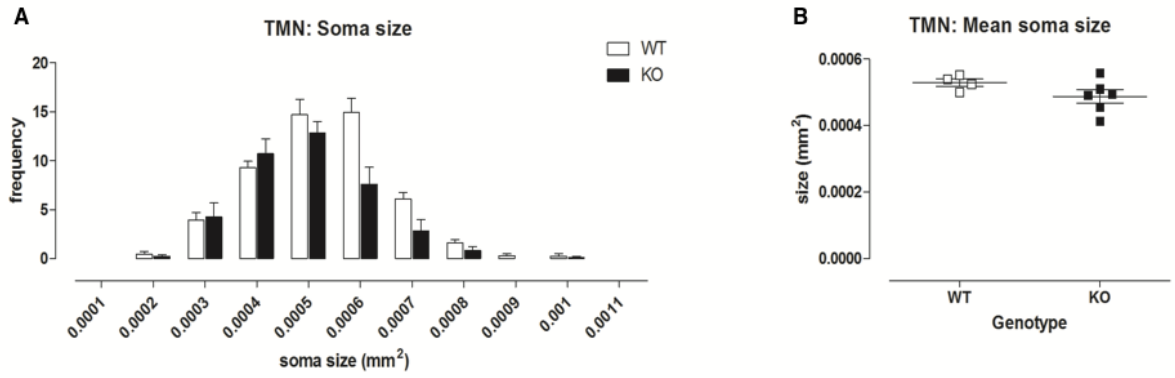

Figure 22. **Frequency distribution (A) and mean soma size (B) in the trigeminal motor nucleus**. The soma size with highest frequency in *Wfs1*$^{-/-}$ mice was 0.0004 mm^2. Although similar, the WT distribution was more broad. However, there was no significance between the two groups. A representation of the same data as the mean values of *Wfs1*$^{-/-}$ and WT mice (B). WT n=4, *Wfs1*$^{-/-}$ (KO) n=6.

2.3.5 DENSITY OF TRIGEMINAL MOTOR AND SENSORY NEURONS

As I saw a reduction in the trigeminal tract area (see above, Fig 19), it was therefore important to understand the 2nd order neurons of this system, the trigeminal sensory neurons and the trigeminal motor neurons, both of which show high expression of WFS1 (Luuk *et al*., 2008). The reduction in the tract area suggests that the number of axons of the trigeminal neurons or the trigeminal motor neurons might be reduced. Density of neurons per nucleus was therefore quantified.

There was no significant decrease in density of either motor or sensory neurons (see Fig. 23). I can therefore suggest that a reduction in number of trigeminal motor neurons does not underlie trigeminal tract size reduction. This reduction may be also due to axon degeneration of the trigeminal neurons, which will form part of future experiments. We know that synaptic density and axonal growth is impaired in cortical cells deficient in WFS1 (Cagalinec *et al*., 2016), therefore this might also apply to the trigeminal neurons also.

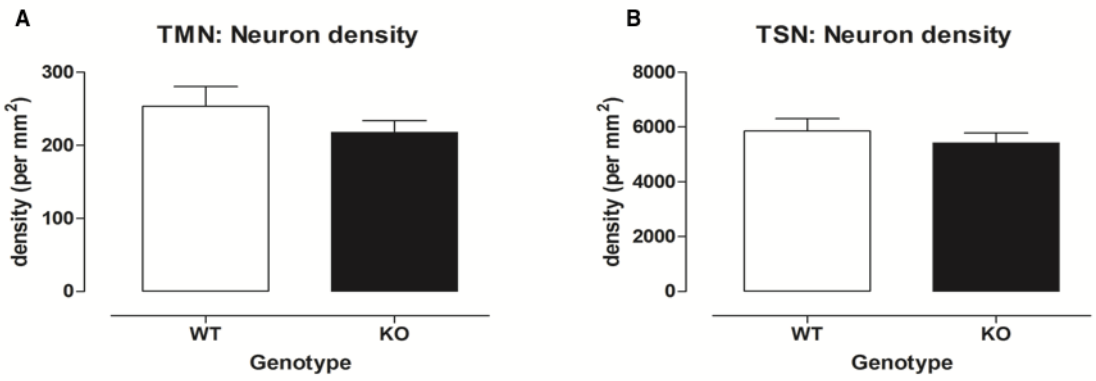

Figure 23. Neuronal density of trigeminal motor neurons (A) and trigeminal sensory neurons (B). No significant reduction in trigeminal motor or sensory neuron density was observed in P22 *Wfs1*$^{-/-}$ mice compared to WT. *Wfs1*$^{-/-}$ (KO) n=6, WT n=4.

In summary, climbing and rearing behaviour in 8-month-old *Wfs1*$^{-/-}$ mice was vastly reduced, suggesting severe disease progression by this age, where we first see MRI evidence of brain stem and trigeminal nerve atrophy. I then went on to examine much younger mice. Based on these data, it can be concluded that brain volume is already affected at very early stages in WS. Total brain stem volume was not significantly reduced in P22 *Wfs1*$^{-/-}$ mice, however, specific components were as I did observe a reduction in spinal trigeminal tract. In cerebellum, I observed a considerable reduction in total volume. Myelin basic protein expression in cerebellar folia was reduced suggesting a degeneration of white matter, where axons of passage traverse. It is now important to further this analysis by examining specific neuronal populations in the cerebellum, in particular, the Purkinje cells, which express WFS1. Given the reduction in trigeminal tract, we need to investigate trigeminal neurons in more detail, and for these experiments, *in vitro* analyses are ideal.

CONCLUSION

Wolfram syndrome causes abnormalities in brain axonal tracts and brain atrophy. Here, I show that the volume of total cerebellum is reduced at very early ages (P22) in *Wfs1*$^{-/-}$ mice. Levels of myelin basic protein in the cerebellum were also greatly reduced suggesting loss of or damage to axonal tracts.

The trigeminal tract, within the pons (brain stem) is also reduced in size in young mice. Total brain stem showed no considerable decrease in volume at this age. The reduction in area of the trigeminal tract suggests a loss in trigeminal neurons or in trigeminal motor neurons, or a loss in axons of either. Myelin content was unchanged. Densities of trigeminal motor and sensory nuclei were not altered in *Wfs1*$^{-/-}$ mice. Soma size of the motor trigeminal neurons showed no considerable change.

Thus, I can conclude that the brain stem and cerebellum is affected at very early stages of WS. As I know from previous research in humans, brain stem volume decreases as the patients age and the results obtained with very young *Wfs1*$^{-/-}$ mice in this work confirmed that there is no significant total volume reduction. However, the loss in cerebellar and possibly white matter at this age suggests a developmental impairment. WS patients show extensive gait deficits, and the cerebellum is particularly important for fine motor control. Furthermore, WS patients develop problems with mastication and also trigeminal neuralgia-like symptoms. Future work will examine the oligodendrocytes (the cells that produce myelin) and trigeminal neurons in detail to work out possible interventions for these abnormalities.

KOKKUVÕTE

Wolframi sündroomi neuropatoloogia ja aju atroofia

Kerli Tulva

Resümee

Wolframi sündroom (WS) on haruldane geneetiliselt päritav haigus, millele puudub ravi. Patsiendid surevad tavaliselt keskeas (Urano, 2016). Sündroomi esmasteks tunnusteks on magediabeet ja nägemisnärvi atroofia. On teada, et juba väga noores eas esineb nii väikeajus kui ka ajutüves atroofia (Hershey *et al*., 2012; Lugar *et al*., 2016). Oluline on välja selgitada, kui varakult algab aju atroofia, et sellest tulenevalt paremini teada haiguse kulgu ja seda mõjutada.

Antud töö eesmärgiks oli uurida väga varaseid aju muutusi WS hiiremudelis, sest eelnevalt tehtud uuringud on näidanud, et vanemad hiired on haiguse progressist sügavalt mõjutatud. Nimelt kaheksakuustel *Wfs1*$^{-/-}$ hiirtel oli MRT-ga leitud nii ajutüves kui kolmiknärvis oluline atroofia ning sellest lähtuvalt analüüsisin ma nende hiirte käitumist, milles selgus, et neil esineb juba palju WS omaseid neuroloogilisi sümptomeid. Seega oli järgmine samm uurida, kui varakult selle haiguse sümptomid ajus alguse saavad. Selleks kasutasin histoloogilisi meetodeid, mis on palju tundlikumad ja detailsemad kui MRT. Uuringud tehti väikeaju ja ajutüve mahu ning väikeaju valgeaine uurimiseks; kolimknärvi rakkude tiheduse, suuruse, aksonite müeliinkihi ja trakti pindala hindamiseks. WS patsientidel esineb tihti kolmiknärvi neuralgia-laadseid sümptomeid, mis tähendab, et selles on tõenäoliseid kahjustusi.

Kaheksakuustel *Wfs1*$^{-/-}$ hiirtel esines aktiivsuse vähenemist, mis võib tuleneda kas dopamiini retseptorite töö langusest (Visnapuu *et al*., 2013) ning sellest tulenevat motivatsiooni langust või ka koordinatsiooniprobleemidest. Seega selles vanuses, kus oleme täheldanud nii ajutüve kui ka kolmiknärvi atroofiat, on hiired tõsiselt kahjustunud ja seega on vajalik uurida nooremaid hiiri.

22 päevastel *Wfs1*$^{-/-}$ hiirtel leiti atroofia väikeajus, millest võib järeldada, et tegu on arenguprobleemiga, mitte degeneratiivse protsessiga. Uuriti ka väikeaju valgeaineti kasutades immunohistokeemilisi meetodit müeliini põhilise valgu hindamiseks ning avastati, et see on oluliselt kahanenud võrreldes metsiktüüpi hiirtega. Seega müeliini vähenemine väikeaju valgeaines on üks põhjuseid, miks väikeaju ruumala on kahanenud, kuid lähemat uuringut

vajavad ka näiteks Purkinje rakud väikeaju molekulaarses rakukihis, sest nendes rakkudes on WFS1 valk kõrgelt ekspresseeritud (Luuk *et al*., 2008). Ajutüves aga suuri erinevusi metsiktüübiga võrreldes polnud. Teine uuring teostati kolmiknärvi trakti, müeliinkihi ja motoorsete ning sensoorsete neuronite hindamiseks. Kolmiknärvi trakti pindala oli vähenenud, mis viitab kas kolmiknärvi neuronite aksonite ja müeliinikihi (sisenevad trakti kaudu) või kolmiknärvi motoorsete neuronite aksonite (väljuvad trakti kaudu) kahanemisele või kahjustusele. Samuti võib olla kahanenud ka sensoorsete ja motoorsete neuronite arv. Kolmiknärvi motoorsetes ja sensoorsetes neuronites on WFS1 valgu ekspressioon kõrge (Luuk *et al*., 2008; Kostakis *et al*., 2008). Trakti müeliinkihis erinevust ei tuvastatud, samuti motoorsete ja sensoorsete neuronite tihedus ja motoorsete närvirakkude suurus ei olnud oluliselt erinev metsiktüüpi hiirtest. Seega vajavad edasist uuringut kolmiknärvid *in vitro*, kus on neid võimalik veelgi detailsemalt uurida.

Varasemalt on meie laboris näidatud WS hiiremudeliga, et WFS1 puudulikkus põhjustab mitokondrite dünaamika vähenemist ja sellest tulenevat närvirakkude degeneratsiooni (Cagalinec *et al*., 2016). Seega on tõenäoline, et WS uurides on võimalik paremini mõista ka teisi mitokondriaalseid neurodegeneratiivseid haigusi. Selles töös saadud tulemused aju atroofia osas aitavad paremini mõista väga varajast haigust ja sellest tulenevalt võimaldavad varajast sekkumist ka patsientides.

REFERENCES

Barrett, T. G., & Bundey, S. E. (1997). Wolfram (DIDMOAD) syndrome. Journal of medical genetics. 34(10): 838-841.

Bathla, G., & Hegde, A. N. (2013). The trigeminal nerve: an illustrated review of its imaging anatomy and pathology. Clinical radiology. 68(2): 203-213.

Bechara, A., Laumonnerie, C., Vilain, N., Kratochwil, C. F., Cankovic, V., Maiorano, N. A., ... & Rijli, F. M. (2015). Hoxa2 selects barrelette neuron identity and connectivity in the mouse somatosensory brainstem. Cell reports. 13(4): 783-797.

Bischoff, A. N., Reiersen, A. M., Buttlaire, A., Al-Lozi, A., Doty, T., Marshall, B. A., & Hershey, T. (2015). Selective cognitive and psychiatric manifestations in Wolfram Syndrome. Orphanet journal of rare diseases. 10(1): 66.

Boutzios, G., Livadas, S., Marinakis, E., Opie, N., Economou, F., & Diamanti-Kandarakis, E. (2011). Endocrine and metabolic aspects of the Wolfram syndrome. Endocrine. 40(1): 10-13.

Cagalinec, M., Liiv, M., Hodurova, Z., Hickey, M. A., Vaarmann, A., Mandel, M., ... & Vasar, E. (2016). Role of Mitochondrial Dynamics in Neuronal Development: Mechanism for Wolfram Syndrome. PLoS Biol. 14(7): e1002511.

Chaussenot, A., Bannwarth, S., Rouzier, C., Vialettes, B., Mkadem, S. A. E., Chabrol, B., ... & Paquis-Flucklinger, V. (2011). Neurologic features and genotype-phenotype correlation in Wolfram syndrome. Annals of neurology. 69(3): 501-508.

Cryns, K., Sivakumaran, T. A., Van den Ouweland, J. M., Pennings, R. J., Cremers, C. W., Flothmann, K., ... & Camp, G. V. (2003). Mutational spectrum of the WFS1 gene in Wolfram syndrome, nonsyndromic hearing impairment, diabetes mellitus, and psychiatric disease. Human mutation. 22(4): 275-287.

Erzurumlu, R. S., Murakami, Y., & Rijli, F. M. (2010). Mapping the face in the somatosensory brainstem. Nature Reviews Neuroscience. 11(4): 252-263.

Fernández-Gil, M. Á., Palacios-Bote, R., Leo-Barahona, M., & Mora-Encinas, J. P. (2010, June). Anatomy of the brainstem: a gaze into the stem of life. In Seminars in Ultrasound, CT and MRI (Vol. 31, No. 3, pp. 196-219). WB Saunders.

Hershey, T., Lugar, H. M., Shimony, J. S., Rutlin, J., Koller, J. M., Perantie, D. C., ... & Washington University Wolfram Study Group. (2012). Early brain vulnerability in Wolfram syndrome. PloS one. 7(7): e40604.

Hickey, M. A., Gallant, K., Gross, G. G., Levine, M. S., Chesselet, M-F. (2005) Early behavioral deficits in R6/2 mice suitable for use in preclinical drug testing. Neurobiology of Disease. 20(1): 1-11

Hickey, M. A., Kosmalska, A., Enayati, J., Cohen, R., Zeitlin, S., Levine, M. S., Chesselet, M-F. (2008) Extensive early motor and non-motor behavioral deficits are followed by striatal neuronal loss in knock-in Huntington's disease mice. Neuroscience. 157(1): 280-295

Hilson, J. B., Merchant, S. N., Adams, J. C., & Joseph, J. T. (2009). Wolfram syndrome: a clinicopathologic correlation. Acta neuropathological. 118(3): 415-428.

Hoekel, J., Chisholm, S. A., Al-Lozi, A., Hershey, T., Tychsen, L., & Washington University Wolfram Study Group. (2014). Ophthalmologic correlates of disease severity in children and adolescents with Wolfram syndrome. Journal of American Association for Pediatric Ophthalmology and Strabismus. 18(5): 461-465.

Hofmann, S., Philbrook, C., Gerbitz, K. D., & Bauer, M. F. (2003). Wolfram syndrome: structural and functional analyses of mutant and wild-type wolframin, the WFS1 gene product. Human molecular genetics. 12(16).

Hurley, R. A., Flashman, L. A., Chow, T. W., & Taber, K. H. (2010). The brainstem: anatomy, assessment, and clinical syndromes. The Journal of neuropsychiatry and clinical neurosciences. 22(1): iv-7.

Inoue, H., Tanizawa, Y., Wasson, J., Behn, P., Kalidas, K., Bernal-Mizrachi, E., ... & Rogers, D. (1998). A gene encoding a transmembrane protein is mutated in patients with diabetes mellitus and optic atrophy (Wolfram syndrome). Nature genetics. 20(2): 143-148.

Karzon, R. K., & Hullar, T. E. (2013). Audiologic and vestibular findings in Wolfram syndrome. Ear and hearing. 34(6): 809.

Kiernan, J. A. (2007). Histochemistry of staining methods for normal and degenerating myelin in the central and peripheral nervous systems. Journal of Histotechnology. 30(2): 87-106.

Kostakis, N. A., Ng, L. L., & Guillozet-Bongaarts, A. L. (2008). Motor Nucleus of the Trigeminal Nerve.

Lin, W., & Popko, B. (2009). Endoplasmic reticulum stress in disorders of myelinating cells. Nature neuroscience. 12(4): 379-385.

Lochhead, J. J., & Thorne, R. G. (2012). Intranasal delivery of biologics to the central nervous system. Advanced drug delivery reviews. 64(7): 614-628.

Lu, S., Kanekura, K., Hara, T., Mahadevan, J., Spears, L. D., Oslowski, C. M., ... & Blanner, P. (2014). A calcium-dependent protease as a potential therapeutic target for Wolfram syndrome. Proceedings of the National Academy of Sciences. 111(49): E5292-E5301.

Lugar, H. M., Koller, J. M., Rutlin, J., Marshall, B. A., Kanekura, K., Urano, F., ... & Washington University Wolfram Syndrome Research Study Group. (2016). Neuroimaging evidence of deficient axon myelination in Wolfram syndrome. Scientific reports. 6.

Luuk, H., Koks, S., Plaas, M., Hannibal, J., Rehfeld, J. F., & Vasar, E. (2008). Distribution of Wfs1 protein in the central nervous system of the mouse and its relation to clinical symptoms of the Wolfram syndrome. Journal of Comparative Neurology. 509(6): 642-660.

Luuk, H., Plaas, M., Raud, S., Innos, J., Sütt, S., Lasner, H., ... & Vasar, E. (2009). Wfs1-deficient mice display impaired behavioural adaptation in stressful environment. Behavioural brain research. 198(2): 334-345.

Montano, N., Conforti, G., Di Bonaventura, R., Meglio, M., Fernandez, E., & Papacci, F. (2015). Advances in diagnosis and treatment of trigeminal neuralgia. Therapeutics and clinical risk management. 11. 289.

Mozzillo, E., Delvecchio, M., Carella, M., Grandone, E., Palumbo, P., Salina, A., ... & Vecchione, G. (2014). A novel CISD2 intragenic deletion, optic neuropathy and platelet aggregation defect in Wolfram syndrome type 2. BMC medical genetics. 15(1): 88.

Pickett, K. A., Duncan, R. P., Hoekel, J., Marshall, B., Hershey, T., & Earhart, G. M. (2012). Early presentation of gait impairment in Wolfram Syndrome. Orphanet journal of rare diseases. 7(1): 92.

Rigoli, L., Lombardo, F., & Di Bella, C. (2011). Wolfram syndrome and WFS1 gene. Clinical genetics. 79(2): 103-117.

Strom, T. M., Hörtnagel, K., Hofmann, S., Gekeler, F., Scharfe, C., Rabl, W., ... & Meitinger, T. (1998). Diabetes insipidus, diabetes mellitus, optic atrophy and deafness (DIDMOAD) caused by mutations in a novel gene (wolframin) coding for a predicted transmembrane protein. Human molecular genetics. 7(13): 2021-2028.

Takeda, K., Inoue, H., Tanizawa, Y., Matsuzaki, Y., Oba, J., Watanabe, Y., ... & Oka, Y. (2001). WFS1 (Wolfram syndrome 1) gene product: predominant subcellular localization to endoplasmic reticulum in cultured cells and neuronal expression in rat brain. Human Molecular Genetics. 10(5): 477-484.

Urano, F. (2016). Wolfram syndrome: diagnosis, management, and treatment. Current diabetes reports. 16(1): 6.

Vincze, A., Mázlo, M., Seress, L., Kormoly, S., Ábraham (2008). H. A correlative light and electron microscopic study of postnatal myelination in the murine corpus callosum. International Journal of Developmental Neuroscience. 26(6): 575–584

Visnapuu, T., Plaas, M., Reimets, R., Raud, S., Terasmaa, A., Kõks, S., ... & Altpere, A. (2013). Evidence for impaired function of dopaminergic system in Wfs1-deficient mice. Behavioural brain research. 244: 90-99.

Books:

Kiernan, J. A., and Rajakumar. N. 2014. Barr's The Human Nervous System: An anatomical Viewpoint, p. 159-164. Chapter 10: Cerebellum. Wolters Kluwer/Lippincott Williams and Wilkins. 10th ed. Baltimore.

Patestas, M. A., Gartner, L. P. 2016. A Textbook of Neuranatomy, p. 325-330. Chapter 17: Cranial Nerves. 2nd ed. Wiley.

Thesis:

Vdovenkova, V. (2016). Magnetic resonance imaging in a mouse model of Wolfram syndrome. (Master's Thesis). University of Tartu, Tartu, Estonia.

Used webpages:

http://www.mayoclinic.org/autosomal-recessive-inheritance-pattern/img-20007457

https://www.ncbi.nlm.nih.gov/genome/tools/gdp

http://gensat.org/imagenavigator.jsp?imageID=93679

http://mouse.brain-map.org/experiment/thumbnails/100048576?image_type=atlas

ACKNOWLEDGMENTS

I am very thankful to my highly recognized and professional supervisor Dr M.A. Hickey for all the assistance, patience, valuable advice and ideas she offered me with my thesis and experiments. I appreciate it very highly as it enabled me to learn a lot through the whole process. I would also like to thank my co-supervisor Tambet Tõnissoo who gave me advice on the editing and drafting my thesis. We thank Dr Külli Jaako for kind donation of secondary antibody.

NON-EXCLUSIVE LICENCE

Non-exclusive licence to reproduce thesis and make thesis public

I, Kerli Tulva
born in 14.10.1994

1. herewith grant the University of Tartu a free permit (non-exclusive licence) to:

1.1. reproduce, for the purpose of preservation and making available to the public, including for addition to the DSpace digital archives until expiry of the term of validity of the copyright, and

1.2. make available to the public via the web environment of the University of Tartu, including via the DSpace digital archives until expiry of the term of validity of the copyright,

Neuropathology and brain atrophy in Wolfram syndrome

supervised by Miriam Ann Hickey and Tambet Tõnissoo

2. I am aware of the fact that the author retains these rights.

3. I certify that granting the non-exclusive licence does not infringe the intellectual property rights or rights arising from the Personal Data Protection Act.

Tartu, 19.04.2017